Hindawi
International Journal of Antennas and Propagation
Volume 2023, Article ID 7622014, 11 pages
https://doi.org/10.1155/2023/7622014

Research Article

A Low Cross-Polarization Microstrip Antenna Array for Millimeter Wave Applications

Yanzhi Fu, Yixiang Lin, and Changda Shi

Shenzhen Academy of Metrology and Quality Inspection, Shenzhen 518073, China

Correspondence should be addressed to Yixiang Lin; linyx@smq.com.cn

Received 16 November 2022; Revised 15 December 2022; Accepted 12 May 2023; Published 6 June 2023

Academic Editor: Jun Xiao

A low cross-polarization microstrip antenna array for millimeter wave (mmW) applications is proposed in this paper. The antenna element is composed of symmetric T-shaped patches with vias. The adoption of a double-sided symmetric radiation patch structure can suppress the cross-polarized electric field, and the vias reduces energy leakage during the power transmission along the antenna patches. To verify the concept, a 1×8 antenna array is fabricated and measured. The measured −10 dB impedance of the antenna array is 28.4% (31 GHz–41.5 GHz) and the peak gain is 15 dBi. The cross polarization ratio is above 35 dB and the 3 dB beamwidths on *E*-plane and *H*-plane are 7.5° and 135°, respectively. The proposed compact size and low cross-polarization antenna array might be a good choice for phased array radar and 5th generation (5G) mobile communication applications.

1. Introduction

In recent years, the millimeter wave (mmW) band has developed vigorously in related technologies and applications due to its rich spectrum resources, especially in 5G big data transmission, radar, and imaging applications. In practical applications, the mmW communication systems pursue easy integration and high reliability. Hence, the antenna designs for mmW applications are also required to possess the characteristics of the compact structure and easy integration.

The mmW antennas using cavity or waveguide structures have been extensively studied due to their low loss [1–3]. However, the big dimensions and weights restrict its applications for large-scale arrays' integration. In contrast, PCB antennas made of low loss dielectric are a good choice for millimeter front-end systems. Many researchers have realized the broadband dual polarization/circular polarization characteristics utilizing multilayer stacking multiple resonance branches/gaps [4–12]. A broadband magnetic electric (ME) dipole antenna with circular polarization operating in the mmW band is proposed in [12]. The rectangular patch is fed through the cross gap of the ground plane to realize the circular polarization. A ME dipole antenna consisting of two patches and a short strip is applied for Ka band [13]. The patch is fed by a rectangular slot on the lower layer of the substrate-integrated waveguide (SIW). The 4×4 array is designed and achieves 5.4 GHz bandwidth (27.7–32.3 GHz) and 15.25 dB gain. There are also studies on single-layer microstrip or SIW type antennas [14–25]. An improved bow tie symmetric dipole linear array antenna with single-layer plate structure is proposed in [25]. Bandwidth of 10.51 GHz (23.41–33.92 GHz) and 10.7 dBi high gain is achieved.

In this paper, a mmW linear array antenna with ground reflection is proposed, and its structure consists of strip lines and double-sided patches. The radiation element consists of a symmetrical T-shaped patch and vias. The antenna is fed by η-type microstrip line. The 1×8 linear array antenna is then designed. The proposed antenna achieves the bandwidth of 10.5 GHz (31 GHz–41.5 GHz, 28.4%) with above 35 dB cross-polarization ratio performance. The 3 dB beamwidth is 7.5° on *E*-plane and the realized gain of the antenna array is over 14.5 dB. Moreover, 135° wide beam characteristic on the *H* plane are also obtained. Therefore, the proposed antenna array possesses a compact structure and would be an excellent candidate for phased array radar and 5G mobile communication applications.

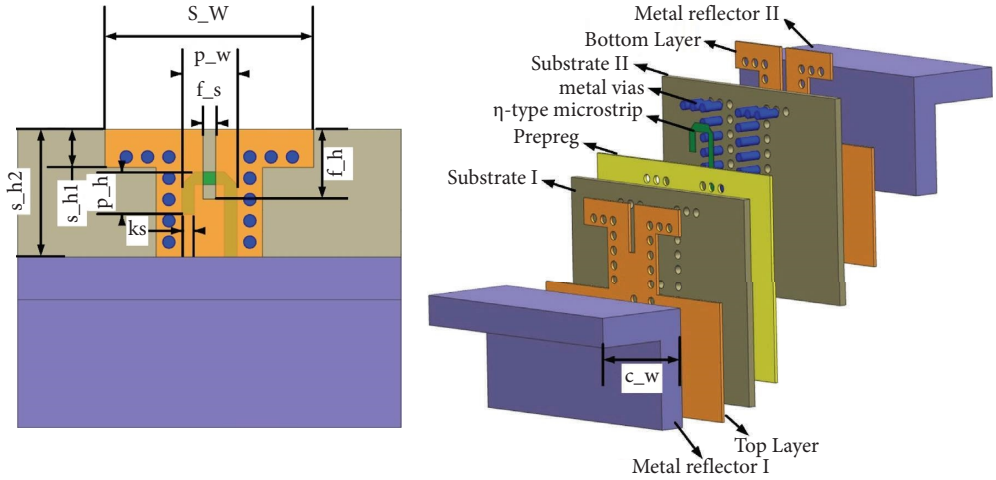

Figure 1: Configuration of antenna element: (a) front view and (b) exploded view.

2. Antenna Element Design

In this paper, the antenna element is designed using Rogers RT Duroid 5880 printed circuit board (PCB). The thickness of the board is 0.254 mm and the dielectric constant is 2.2. The antenna radiation element adopts a double-sided symmetrical T-shaped structure with a rectangular groove, as shown in Figure 1. An η-type microstrip in the middle of the two PCB layers is introduced acting as the coupling fed structure. A reflective ground plane is introduced at the bottom of the antenna element to suppress the back radiation, thus reducing the antenna back lobe. The distance from the top of the antenna to the reflector s_h2 is usually a quarter of the wavelength, which increases the realized gain of the antenna element by making the reflective electric field cophase stacking, as shown in Figure 2. The vias along the dipoles is proposed to reduce the energy diffusion within the substrates. The energy diffusion in the ineffective area of the microstrips is significantly reduced, as shown in Figure 3. The reduction of ineffective energy diffusion is beneficial to reduce the coupling effect between the antenna inner feeding network and other circuits within the overall system, especially in the millimeter wave band. The double-sided symmetrical structure can effectively eliminate the cross-polarization electric field and therefore improves the cross-polarization performance of the antenna. It is because the cross-polarization displacement current generated between the feed microstrip and double-layer patches in the double-sided symmetrical structure is offset by the equal magnitude and the opposite vector direction, while the single-layer PCB board structure is not. The cross-polarized electric field distributions of single-layer and double-layer radiation patches are shown in Figure 4. It is obvious that the electric field energy at the radiation interface of double-layer patches is significantly smaller. Also, the cross-polarization of double-layer patches is about 20 dB lower than the single-layer patch, as shown in Figure 5. Through optimization, the parameters of the antenna element have to be optimized and are listed in Table 1.

The length scanning result of the parameter f_h is shown in Figure 7. The parameter f_h mainly affects the impedance bandwidth matching of the antenna and the resonant frequency. According to the optimization results, the parameter f_h is selected as 1.64 mm. The antenna element achieves a bandwidth of 12.5 GHz, and the impedance bandwidth ratio is 33.8% at 37 GHz.

The surface current distributions of different resonant frequencies are shown in Figure 8. It can be found that the vias avoids the diffusion of the energy inside the plate. The vias can also provide an extended path for the T-shaped patch. The copolarization and cross-polarization patterns of the antenna element at 37 GHz are shown in Figure 9. The antenna gain reaches 6.83 dB, and the 3 dB beamwidth on E-plane is 68°, the beamwidth on H-plane is 135°, and the cross-polarization ratio is 40 dB.

On one hand, the reflector plane reflects back radiation energy and superposes it with the forward propagated energy. Theoretically, the distance is 1/4 wavelength of the central frequency, which achieves the in-phase superposition. On the other hand, the antenna gain is the largest, while the 3 dB beam width is the smallest. At 37 GHz, the 1/4 wavelength is 2 mm. Comparison of H-plane pattern versus s_h2 (varying from 2 mm to 4 mm) is shown in Figure 10, where s_h2 is the distance from the antenna aperture to the reflector plane. When s_h2 is 2 mm, the maximum gain of the antenna element is 8.2 dB, while the 3 dB beamwidth is the minimum 91.5°. The gain decreases as s_h2 becomes larger, while the beam width is broadened. According to the optimization process, s_h2 is set as 3 mm and c_w is set as 3.5 mm.

3. Antenna Array Design

A mmW linear array antenna with dual side dipoles of the microstrip structure is shown in Figure 11. A 1×8 linear array antenna is designed. The distance between the nearby elements is 7 mm. Structure of the feed network is shown in Figure 12. The energy diffusion in the ineffective area of the

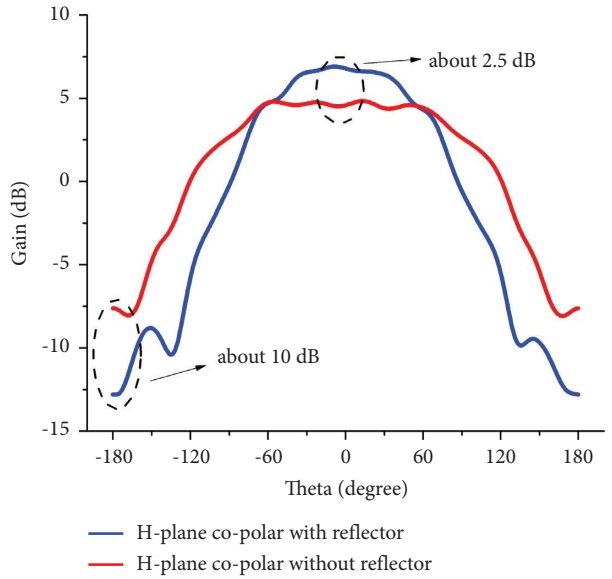

Figure 2: Comparison of radiation patterns of the antenna with and without reflective ground plane.

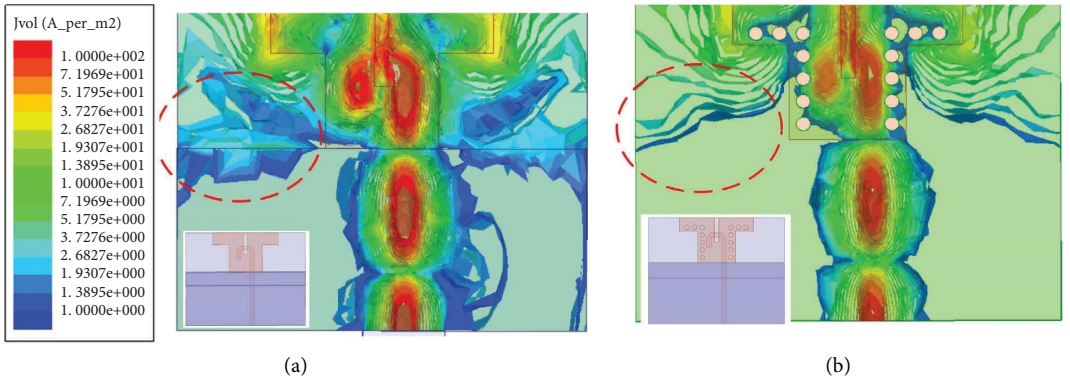

Figure 3: Comparison of the electric field of antenna element: (a) without vias and (b) vias.

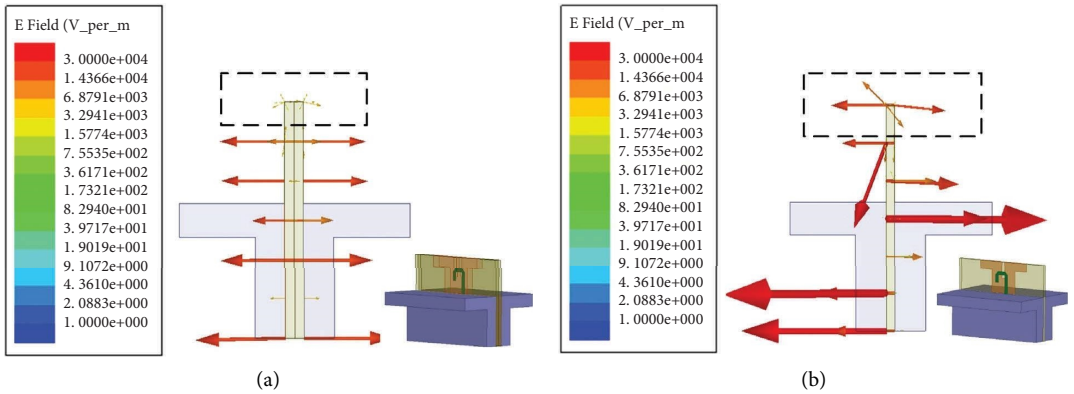

Figure 4: Cross-polarized electric field distribution: (a) double-layer radiation patch and (b) single-layer radiation patch.

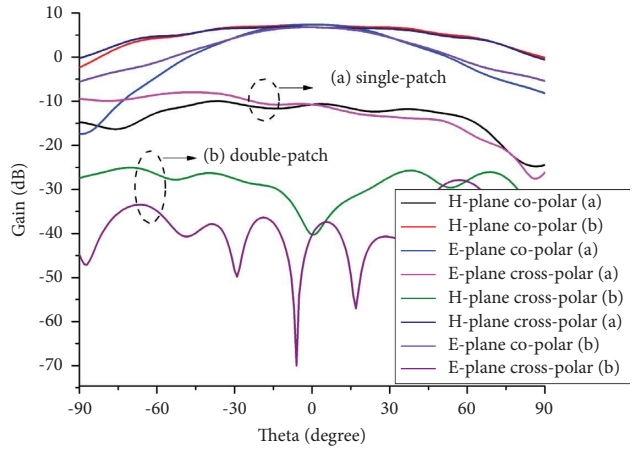

Figure 5: Comparison of radiation patterns of the single-patch and double-patch structures.

Table 1: Antenna structural parameters and dimensions.

Name	s_w	p_w	f_s	f_h	s_h1	s_h2	p_h	ks	c_w
Value	4.9	1.3	0.3	1.64	0.9	3.0	1	0.3	3.5

Note that the parameter s_w affects the resonant frequency of the antenna. The parameter p_h is the length of η-type feeding microstrip and f_h is the length of the rectangular groove. The parameter p_h mainly affects the resonant frequency of the antenna. In order to obtain the 37 GHz resonant frequency and meet the bandwidth characteristics requirement, p_h = 1 mm is set. The S_{11} versus parameter p_h is shown in Figure 6. Unit: mm.

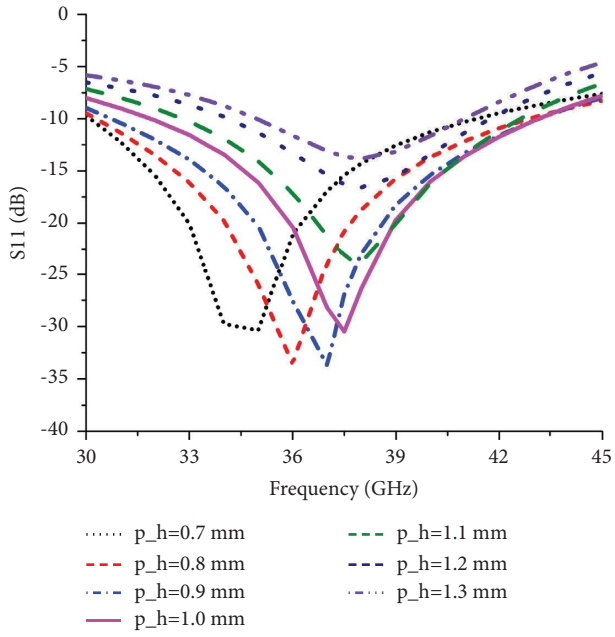

Figure 6: S_{11} scanning comparison of p_h.

feed network is significantly reduced by adding metallic vias, as shown in Figure 13, and the transmission coefficient of the feed network with metallic vias is shown in Figure 14. The overall dimension of the antenna array is only 58 mm × 9.3 mm if the transition structure from microstrip to coaxial line is not considered. Snap of the proposed antenna array is shown in Figure 15. The microstrip feeding port can be easily integrated with the transmitter and receiver (T-R) component.

4. Antenna Simulation and Measurement

The simulation and measurement results of VSWR for the antenna array are shown in Figure 16. The antenna array achieves the bandwidth of 10.5 GHz (31 GHz–41.5 GHz, VSWR ≤ 2).

Figure 17 shows the simulated and measured patterns of the antenna at 31 GHz, 37 GHz, and 41 GHz. It can be seen that the simulated results are compatible with the measured results. The proposed antenna has above 35 dB cross-

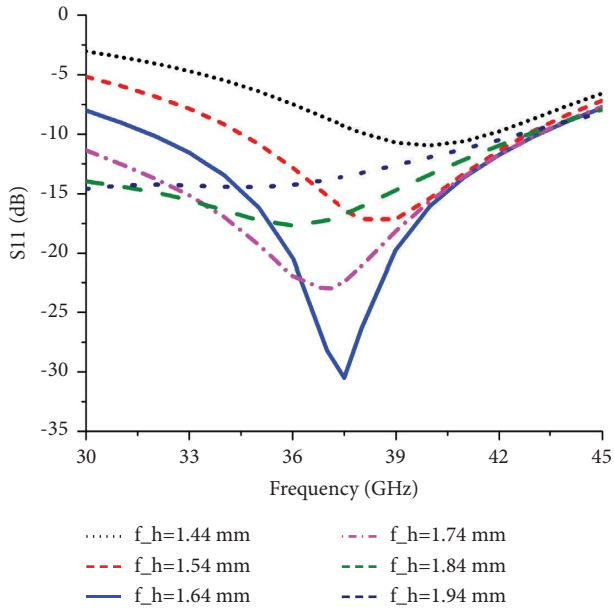

Figure 7: f_h parameter S_{11} scanning comparison diagram.

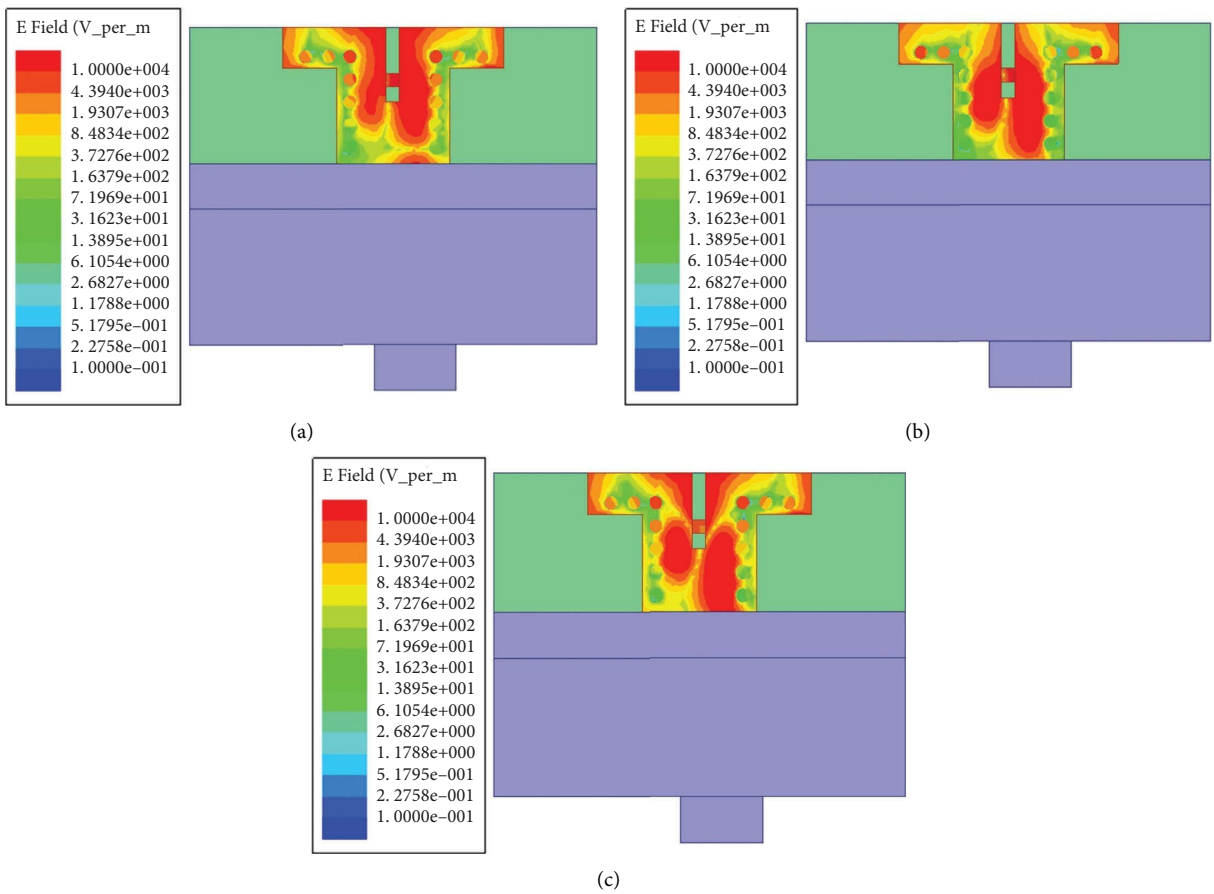

Figure 8: Surface current distribution for the proposed antenna: (a) 32 GHz, (b) 37 GHz, and (c) 43 GHz.

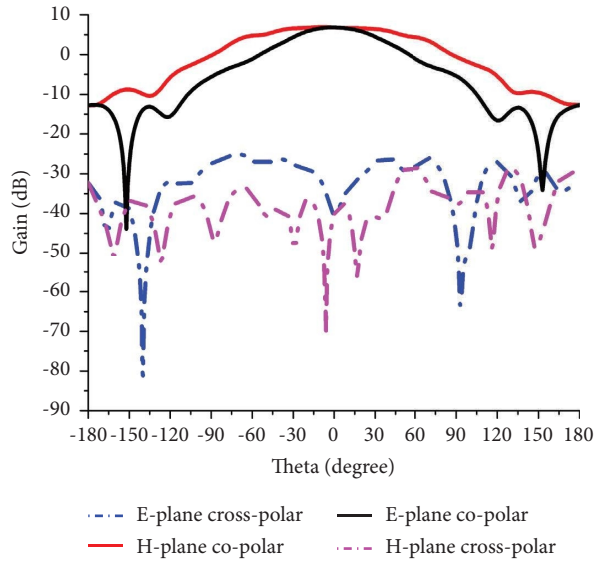

Figure 9: The cross-polarized and copolarized patterns for the antenna elements in *E*-plane and *H*-plane.

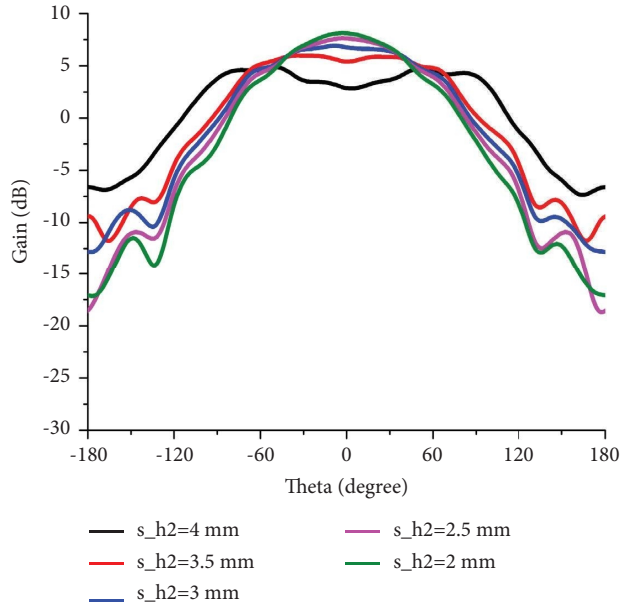

Figure 10: The comparison of the gain *vs.* parameter s_h2.

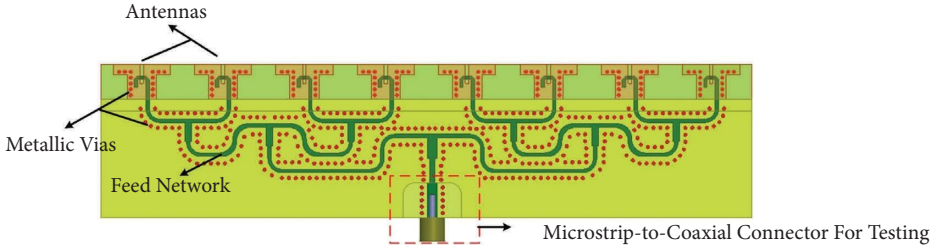

(a)

Figure 11: Continued.

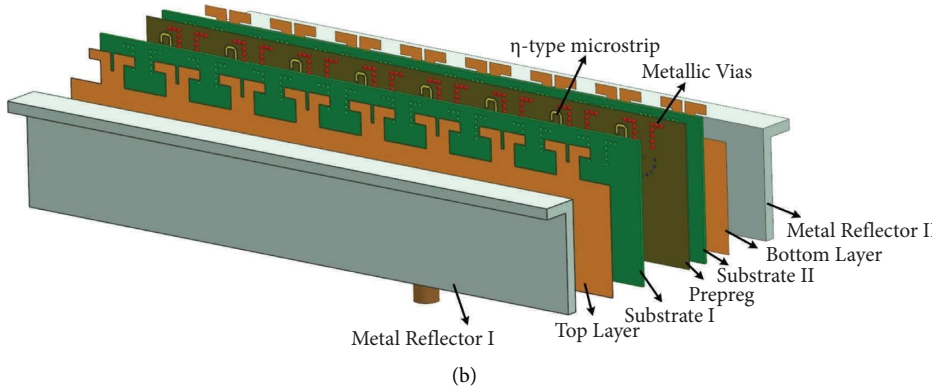

Figure 11: Antenna structure: (a) perspective view and (b) exploded view.

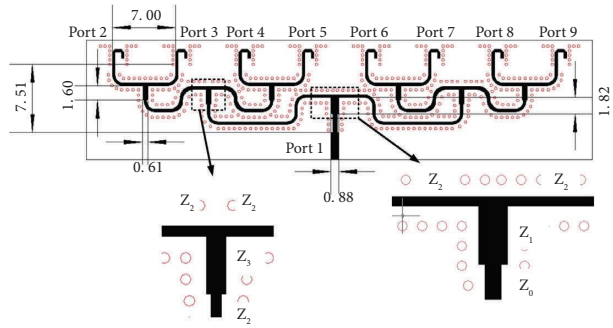

Figure 12: Dimension drawing of feed network structure. ($Z_0 = 50\,\Omega$, $Z_1 = 33.2\,\Omega$, $Z_2 = 68\,\Omega$, and $Z_3 = 46.7\,\Omega$).

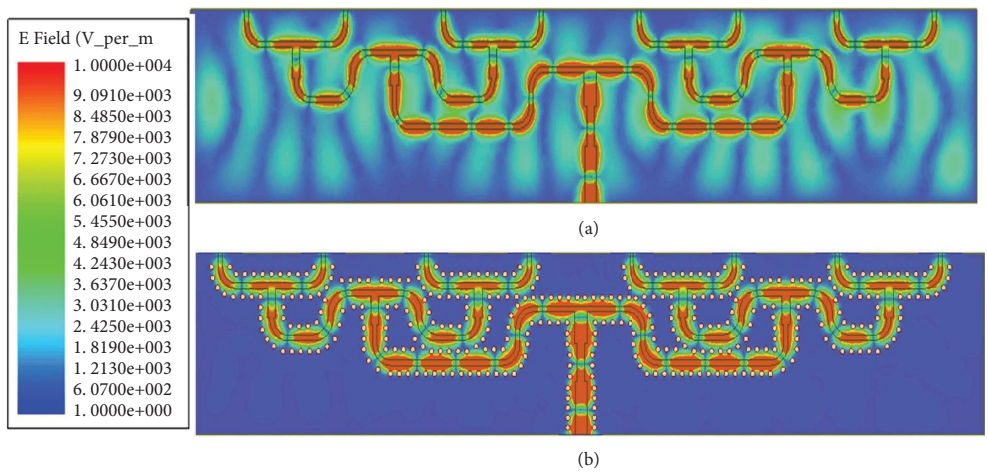

Figure 13: Comparison of the electric field of feed network: (a) without vias and (b) with vias.

polarization performance in the whole operating frequency band. The *E*-plane pattern has a 3 dB beamwidth of 7.5° an a side lobe level of −13 dB, while the *H*-plane pattern has a wide beam width of 135°. Figure 18 shows the simulation and measurement results of antenna gain. The proposed antenna has a high gain of 15 dB.

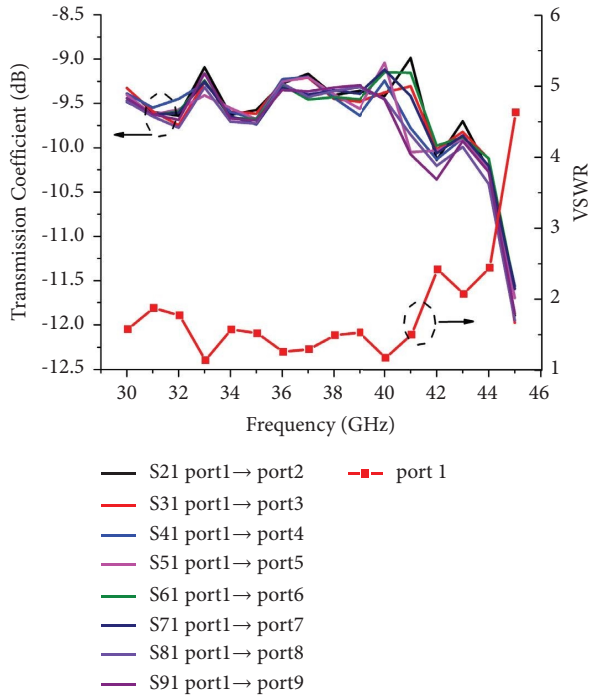

Figure 14: Transmission coefficient of the feed network with vias. (The port serial numbers are the same as in Figure 11).

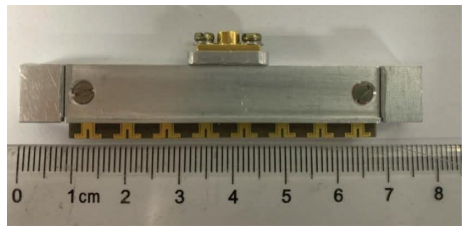

Figure 15: Snap of the proposed antenna array.

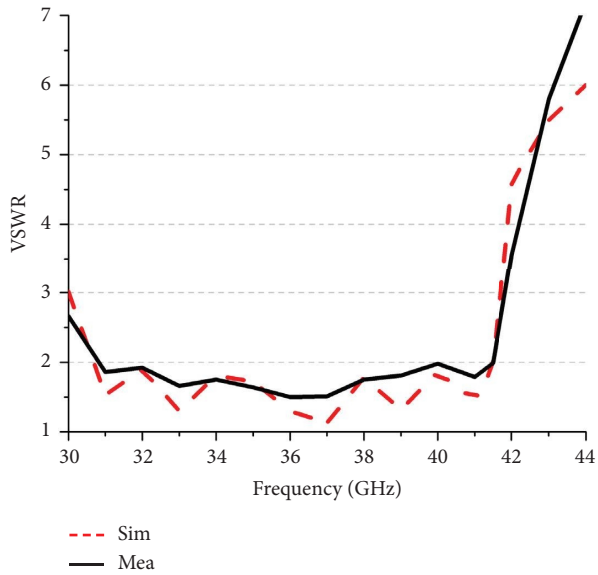

Figure 16: The simulation and measurement results of the antenna VSWR.

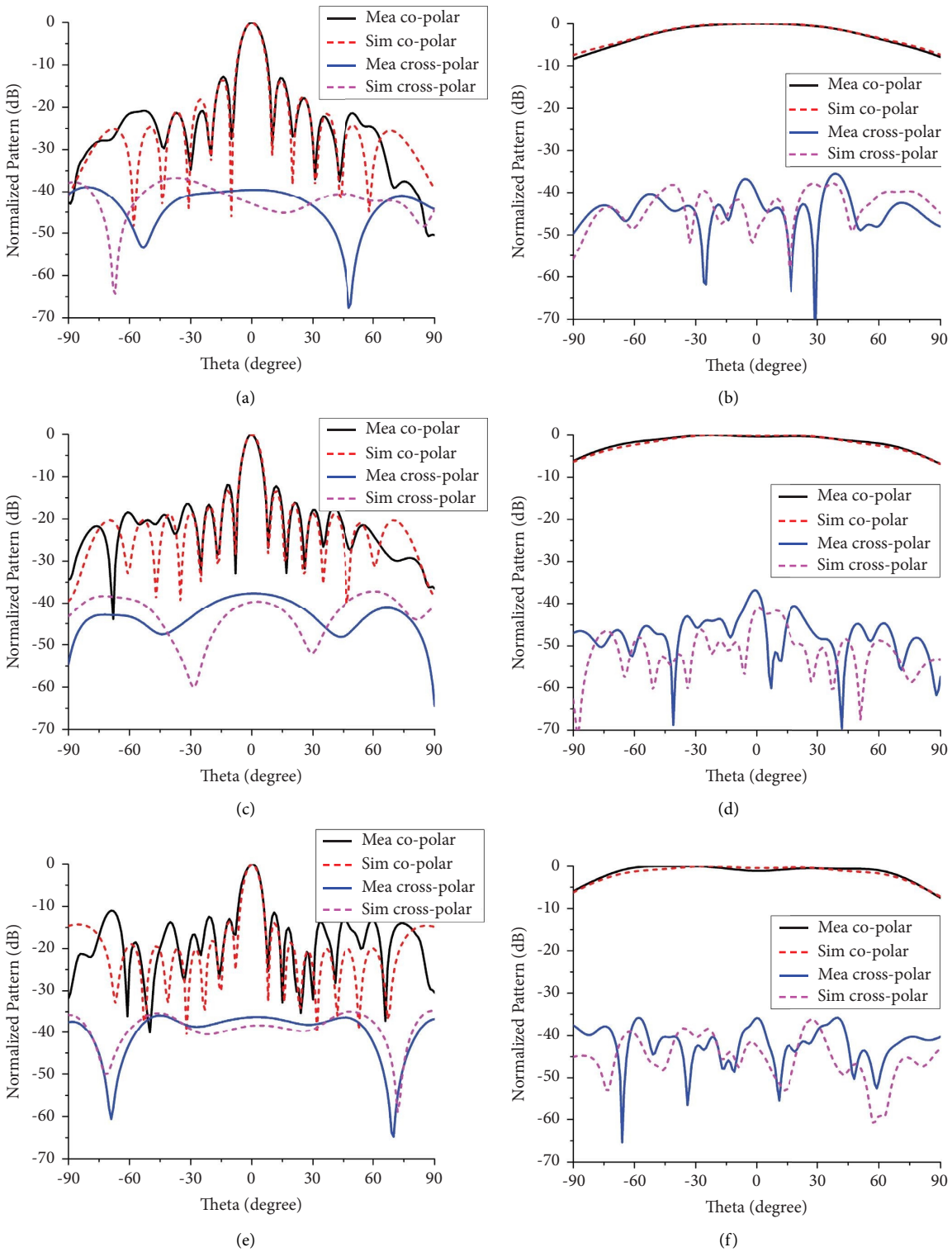

FIGURE 17: Simulated and measured patterns: (a) *E*-plane, 31 GHz; (b) *H*-plane, 31 GHz; (c) *E*-plane, 37 GHz; (d) *H*-plane, 37 GHz; (e) *E*-plane, 41 GHz; and (f) *H*-plane, 41 GHz.

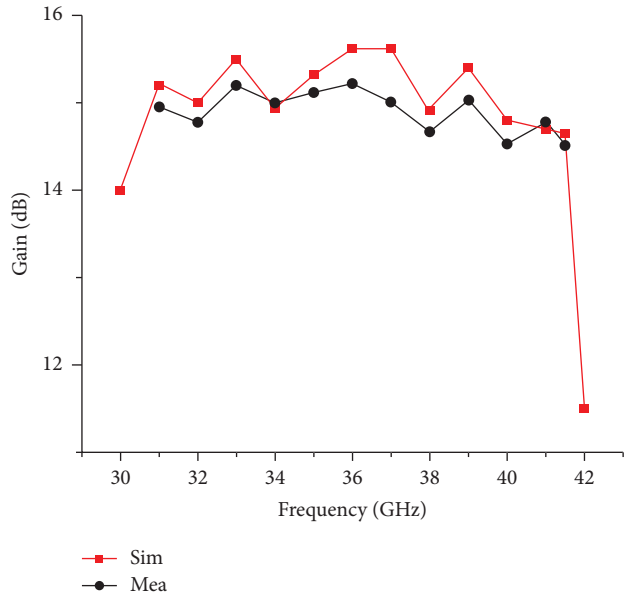

Figure 18: Antenna gain.

5. Conclusions

In this paper, a T-shaped linear array antenna with reflective ground operating at the mmW band is proposed. Protype measurement of the antenna shows that in the bandwidth of 10.5 GHz (31 GHz–41.5 GHz), stable high gain and good radiation pattern characteristics can be obtained. Moreover, the antenna realized a compact size with low cross-polarization. The proposed antenna is suitable for mmW band-phased array applications and 5G communication.

Data Availability

All data, models, and code generated or used during the study are included within the article.

Conflicts of Interest

The authors declare that they have no conflicts of interest.

Acknowledgments

This study was funded by Open Research Fund Project of State Key Laboratory of Market Regulation (Quality Infrastructure Efficiency field) (Grant No. KF20220201), Science and Technology Program of State Administration for Market Regulation (Grant Nos. 2022MK144, 2022MK143, and 2021MK129), and SMQ mmW Laboratory Testing Capacity Enhancement Project.

References

[1] F. Sun, Y. Li, J. Wang, L. Ge, J. Chen, and W. Qin, "Bandwidth enhancement of millimeter-wave large-scale antenna arrays using X-type full-corporate waveguide feed networks," *IEEE Open Journal of Antennas and Propagation*, vol. 3, pp. 1044–1056, 2022.

[2] Z. Liu, H. Lu, J. Liu, S. Yang, Y. Liu, and X. Lv, "Compact fully metallic millimeter-wave waveguide-fed periodic leaky-wave antenna based on corrugated parallel-plate waveguides," *IEEE Antennas and Wireless Propagation Letters*, vol. 19, no. 5, pp. 806–810, May 2020.

[3] J. Fan, "Millimeter-wave multimode beamforming network based on double-ridged waveguides," in *Proceedings of the 2021 International Conference on Microwave and Millimeter Wave Technology (ICMMT)*, pp. 1–3, Nanjing, China, May 2021.

[4] C.-E. Tsai, H. Jin, C. H. Liao et al., "A 60 GHz rhombic patch array antenna with high gain, low sidelobe level, and reduced array area," *IEEE Access*, vol. 10, pp. 86498–86509, 2022.

[5] Z. Ji, G.-H. Sun, and H. Wong, "A wideband circularly polarized complementary antenna for millimeter-wave applications," *IEEE Transactions on Antennas and Propagation*, vol. 70, no. 4, pp. 2392–2400, 2022.

[6] X. Dai and K. M. Luk, "A wideband dual-polarized antenna for millimeter-wave applications," *IEEE Transactions on Antennas and Propagation*, vol. 69, no. 4, pp. 2380–2385, 2021.

[7] C. Zhao, "Broadband dual polarization antenna array for 5G millimeter wave applications," in *Proceedings of the 2019 International Symposium on Antennas and Propagation (ISAP)*, pp. 1–3, Xi'an, China, April 2019.

[8] J. Sun and K.-M. Luk, "Wideband magneto-electric dipole antennas for millimeter-wave applications with microstrip line feed," in *Proceedings of the 2018 International Symposium on Antennas and Propagation (ISAP)*, pp. 1-2, Busan, South Korea, October 2018.

[9] X. Tong, Z. H. Jiang, C. Yu, F. Wu, X. Xu, and W. Hong, "Low-profile, broadband, dual-linearly polarized, and wide-angle millimeter-wave antenna arrays for ka-band 5G applications," *IEEE Antennas and Wireless Propagation Letters*, vol. 20, no. 10, pp. 2038–2042, 2021.

[10] Q. Li, Y. Zhang, and W. Hong, "Broadband patch loaded substrate-integrated cavity backed slot array for millimeter-wave applications," in *Proceedings of the 2021 IEEE International Symposium on Antennas and Propagation and USNC-URSI Radio Science Meeting (APS/URSI)*, pp. 1677-1678, Singapore, December 2021.

[11] Y. He, S. Lv, L. Zhao, G.-L. Huang, X. Chen, and W. Lin, "A compact dual-band and dual-polarized millimeter-wave beam scanning antenna array for 5G mobile terminals," *IEEE Access*, vol. 9, pp. 109042–109052, 2021.

[12] J. Li, Y. Hu, L. Xiang, W. Kong, and W. Hong, "Broadband circularly polarized magnetoelectric dipole antenna and array for K-band and ka-band satellite communications," *IEEE Transactions on Antennas and Propagation*, vol. 70, no. 7, pp. 5907–5912, July 2022.

[13] Z. Tang and Y. Dong, "A ka-band antenna array based on wide-beamwidth magnetoelectric dipole," *IEEE Antennas and Wireless Propagation Letters*, vol. 21, no. 3, pp. 501–505, 2022.

[14] B.-K. Tan, S. Withington, and G. Yassin, "A compact microstrip-fed planar dual-dipole antenna for broadband applications," *IEEE Antennas and Wireless Propagation Letters*, vol. 15, pp. 593–596, 2016.

[15] X. Wang, Z. Chen, Y. Yao, L. Qi, J. Yu, and X. Chen, "A SIW based millimeter-wave slot antenna with circular polarization," in *Proceedings of the 2018 International Conference on Microwave and Millimeter Wave Technology (ICMMT)*, pp. 1–3, Chengdu, China, December 2018.

[16] P. Kumawat and S. Joshi, "Review of Slotted SIW antenna at 28 GHz and 38 GHz for mm-wave applications," in *Proceedings of the 2020 12th International Conference on*

Computational Intelligence and Communication Networks (CICN), pp. 8–13, Bhimtal, India, January 2020.

[17] L. Zhang, Y. He, S.-W. Wong, and S. Gao, "Millimeter-wave wideband circularly polarized antenna array using SIW-fed S-dipole elements," in *Proceedings of the 2019 IEEE International Symposium on Antennas and Propagation and USNC-URSI Radio Science Meeting*, pp. 1231-1232, Atlanta, GA, USA, June 2019.

[18] Y. Zhang, J.-Y. Deng, D. Sun, J. Y. Yin, and L. X. Guo, "Compact slow-wave SIW H-plane horn antenna with increased gain for vehicular millimeter wave communication," *IEEE Transactions on Vehicular Technology*, vol. 70, no. 7, pp. 7289–7293, 2021.

[19] W.-H. Zhang, L. Ke, S. Liao et al., "Low-profile broadband vertically polarized microstrip magnetic dipole antenna with endfire radiation," *IEEE Antennas and Wireless Propagation Letters*, vol. 20, no. 10, pp. 2003–2007, 2021.

[20] D. Lee and A. B. Yakovlev, "Metasurface cloaks to decouple closely spaced printed dipole antenna arrays fed by a microstrip-to-balanced transmission-line transition," *IEEE Access*, vol. 9, pp. 128209–128219, 2021.

[21] J. Wang, Y. Li, F. Wu, D. Jiang, and J. Wang, "Millimeter-wave wideband endfire magnetoelectric dipole antenna fed by substrate integrated coaxial line," *IEEE Transactions on Antennas and Propagation*, vol. 70, no. 3, pp. 2301–2306, March 2022.

[22] K. Trzebiatowski, M. Rzymowski, L. Kulas, and K. Nyka, "Simple 60 GHz switched beam antenna for 5G millimeter-wave applications," *IEEE Antennas and Wireless Propagation Letters*, vol. 20, no. 1, pp. 38–42, 2021.

[23] J. Yang, Y. Shen, L. Wang, H. Meng, W. Dou, and S. Hu, "2-D scannable 40-GHz folded reflectarray fed by SIW slot antenna in single-layered PCB," *IEEE Transactions on Microwave Theory and Techniques*, vol. 66, no. 6, pp. 3129–3135, June 2018.

[24] Y. Cheng and Y. Dong, "Wideband circularly polarized planar antenna array for 5G millimeter-wave applications," *IEEE Transactions on Antennas and Propagation*, vol. 69, no. 5, pp. 2615–2627, 2021.

[25] H. Ullah and F. A. Tahir, "A high gain and wideband narrow-beam antenna for 5G millimeter-wave applications," *IEEE Access*, vol. 8, pp. 29430–29434, 2020.